



PERSPECTIVE

OPEN ACCESS

RECEIVED
28 April 2020

REVISED
19 June 2020

ACCEPTED FOR PUBLICATION
9 July 2020

PUBLISHED
29 July 2020

Original content from this work may be used under the terms of the [Creative Commons Attribution 4.0 licence](#). Any further distribution of this work must maintain attribution to the author(s) and the title of the work, journal citation and DOI.



Printing and coating MXenes for electrochemical energy storage devices

Sina Abdolhosseinzadeh^{1,2} , Jakob Heier¹ and Chuanfang (John) Zhang^{1,3}

¹ Laboratory for Functional Polymers, Swiss Federal Laboratories for Materials Science and Technology (Empa), Überlandstrasse 129, Dübendorf CH-8600 Switzerland

² Institute of Materials Science and Engineering, Ecole Polytechnique Fédérale de Lausanne (EPFL), Station 12, Lausanne CH-1015 Switzerland

³ Author to whom any correspondence should be addressed.

E-mail: chuanfang.zhang@empa.ch

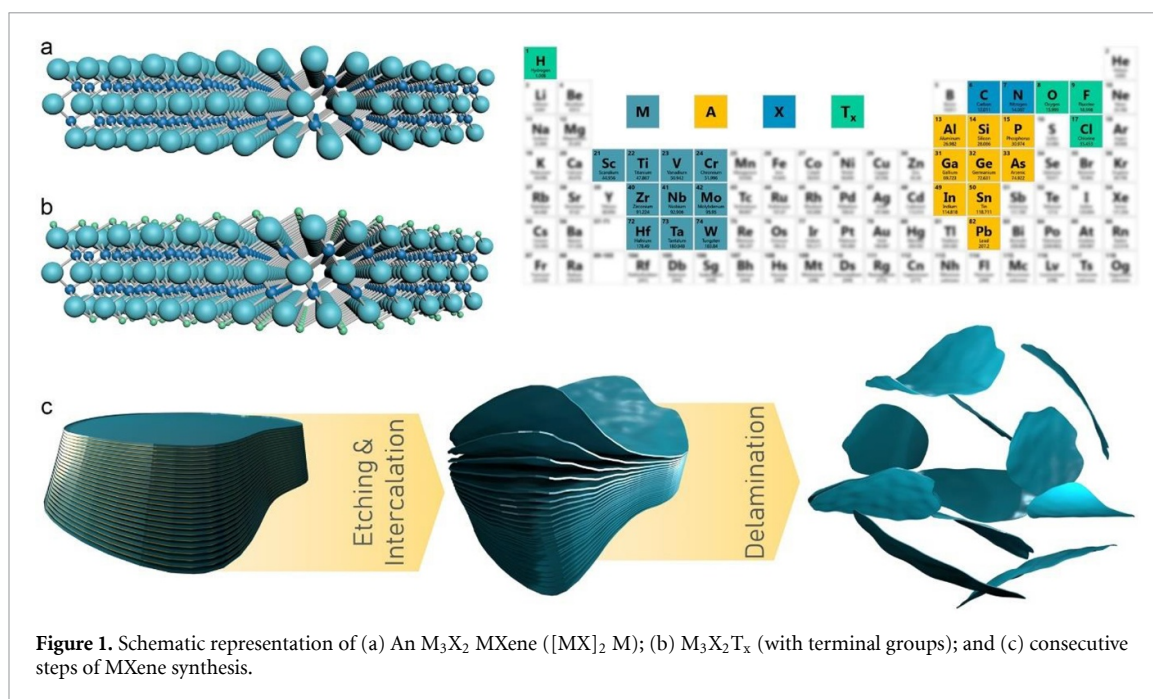
Keywords: printing, coating, ink formulation, MXene, battery, supercapacitor

1. Introduction

In recent years, due to the increased utilization of electrical energy in all aspects of daily life, a huge demand for energy storage systems, for both mobile and stationary applications, has emerged. Electrochemical energy storage devices (EESDs) such as batteries and supercapacitors are the most dominant types of such systems which are usually processed from a liquid phase. Simplicity, low cost, high production yield, and ease of scale-up are some of the main reasons which render the liquid-phase techniques preferable to other fabrication methods. In these methods, a printing or a coating technique is usually used for deposition of a suspension/solution which contains the electrochemically active material. This suspension/solution is called 'ink' and typically contains other additives to facilitate the deposition and film formation processes. Binders, surfactants, and rheology modifiers are some of the key additives of conventional ink formulations [1]. Although additives play critical roles in the processability of the inks and properties of the printed/coated films, their removal (after drying of the film) is necessary for recovering the functionality of the printed/coated materials. Additives intensively degrade the electrical properties, decrease the active surface area, and complicate the fabrication process as their removal requires high-temperature heat treatments. In order to mitigate the undesirable effects of additives on functionality of the liquid processed materials, numerous methods such as application of localized short/pulsed heating techniques [2] and replacing the conventional additives with innovative alternatives like solvent mixtures [3] have been established. Although great attempts have been made, most of the proposed solutions are case-specific, with limited scope of application.

Recently, MXenes, a new class of two-dimensional materials, have been discovered by Gogotsi, Barsoum and other researchers at Drexel university [4] which can fundamentally alter the liquid-phase processing of EESDs and address the aforementioned problems. MXenes are layered transition metal carbides, carbonitrides, and nitrides. They have proven to hold great promise not only for EESDs but also for numerous applications such as printed electronics [5–7] thanks to their excellent conductivity and rich surface chemistry. MXenes have a general formula of $M_{n+1}X_n$ (M represents an early transition metal and X is carbon and/or nitrogen), where $n + 1$ layers of M cover n layers of X in an $[MX]_nM$ arrangement (figure 1(a)) [8]. It is noteworthy that MXenes with more than one metallic element, either as solid solutions or ordered phases, have also been successfully realized [9]. Due to the dangling bond passivation of the outermost M layers, the surfaces of MXenes are terminated with abundant functional groups (e.g. $-F$, $-O$, $-OH$, or their combination; figure 1(b)) [10]. Hence, it is more appropriate to describe their chemical formula as $M_{n+1}X_nT_x$ in which, T represents the corresponding terminal group(s).

The functional groups have paramount effects on physical and chemical properties of MXenes; however, unlike functionalized graphenes (e.g. graphene oxide) [11], MXenes can still offer very high conductivities even after terminating their surface with abundant functionalities [8]. Simultaneously being conductive and having high concentrations of surface functional groups, has made MXenes a unique choice for room-temperature liquid-phase-processing. MXene flakes are negatively charged with a zeta potential between -30 and -80 mV [12] which gives them an exceptional colloidal stability in aqueous and polar



solvents. As a result, stable suspensions of MXenes with solid loadings of less than 0.02 to 70 wt.% can be easily prepared without addition of any surfactant [13]. Furthermore, the terminal groups, by establishing hydrogen ($-OH/-F$ or $-OH/-O$) or van der Waals ($-F/-F$ or $-F/-O$) bonds, play a crucial role in interparticle interactions [8] and consequently in film formation processes, mechanical integrity of the films and, their adhesion to the substrates. Hence, the need for binders is eliminated and additive-free MXene inks can be easily formulated. It is notable that the dispersibility of MXenes in various polar solvents enables ink formulation with wide range of surface tensions. In addition to the conventional additives (i.e. surfactants, binders, rheology modifiers, ...), MXenes, owing to their electrochemical activity and superb conductivity may replace other components of the EESD electrode fabrication inks (e.g. conductive binders) which usually unnecessarily increase the device weight [10]. While numerous excellent reviews on electrochemical properties of MXenes and their application in EESDs are available [14–16], very little attention has been paid to the processing of these materials and device fabrication methods. In this perspective, after a brief introduction on MXenes and their synthesis methods, some of the most recent studies on ink formulation and liquid-phase processing of MXenes for fabrication of EESDs have been reviewed.

2. MXenes: definition and synthesis methods

Similar to other 2D materials, MXenes can be synthesized both by bottom-up and top-down approaches; however, because of higher production capacity and lower cost, exfoliation of their parent layered crystals (top-down) is of greater interest (figure 1(c)). Nevertheless, unlike other 2D materials such as graphene, where layers are stacked by weak van der Waals attractions [17], in MXenes, the stack of $M_{n+1}X_n$ layers are interleaved by additional layers with strong metallic bonds [8]. When the additional layer is a monoatomic single layer (designated by word 'A'; an element from group 13 and 14 of the periodic table), the parent crystal is called MAX phase (e.g. Ti_3AlC_2). To synthesize single layers of MXene from the MAX phase, the 'A' layers should be removed. The synthesis of MXenes from non-MAX phases involves removal of diatomic multi layers such as Al_3C_3 from $Zr_3Al_3C_5$ for production of Zr_3C_2 [18]. In both cases, due to the higher chemical activity of the mentioned layers, the removal can be easily done by means of a selective etching agent.

As quality and most of the properties of MXenes (from mechanical to chemical) heavily depend on their synthesis method [8], a great amount of effort has been devoted to the development of different etching techniques. For instance, type and ratio of the functional groups as well as the structural defect density of the nanosheets are mainly determined by the etching method and its conditions [19–21]. Some of the most important and widely used approaches are summarized in table 1. Aqueous solutions of hydrofluoric (HF) acid, owing to their excellent selectivity, have been predominantly used for removal of the 'A' element. Due to the hazardous nature of HF acid and difficulties in its handling, alternative techniques based on mixtures of fluoride salts and strong acids, capable of *in-situ* forming the HF, have been recently developed (e.g. $LiF + HCl$) [22]. Other milder etching agents such as ammonium hydrogen difluoride, ammonium fluoride

Table 1. Summary of MXene synthesis methods.

Etching method	Precursor/MXene	Details and remarks	Ref. #
Aqueous HF solution	$\text{Ti}_3\text{AlC}_2/\text{Ti}_3\text{C}_2\text{T}_x$	50% HF	[4]
Strong acid + fluoride salt	$\text{Ti}_3\text{AlC}_2/\text{Ti}_3\text{C}_2\text{T}_x$	6 M HCl + LiF; Results in larger flakes; no intercalation step is needed	[22]
NH_4HF_2	$\text{Ti}_3\text{AlC}_2/\text{Ti}_3\text{C}_2\text{T}_x$	1 M NH_4HF_2 @60 °C for 8 h	[23]
NH_4F	$\text{Ti}_3\text{AlC}_2/\text{Ti}_3\text{C}_2\text{T}_x$	$\text{NH}_4\text{F}:\text{Ti}_3\text{AlC}_2$ mass ratio 100:1; Hydrothermal etching in autoclave @180 °C for 24 h	[24]
Alkali etching	$\text{Ti}_3\text{AlC}_2/\text{Ti}_3\text{C}_2\text{T}_x$	27.5 M NaOH; Fluorine-free hydrothermal etching in autoclave @270 °C under Ar atmosphere; Functional groups are –O and –OH	[25]
Ionothermal etching	$\text{Ti}_3\text{AlC}_2/\text{Ti}_3\text{C}_2$	Water-free; Safe and low-cost method; Etching in a mixture of Choline chloride/Oxalic acid/ NH_4F @120 °C for 24 h	[26]
Molten fluoride salt	$\text{Ti}_4\text{AlN}_3/\text{Ti}_4\text{N}_3$	KF + LiF + NaF mass ratio of 0.59:0.29:0.12 @ 550 °C under Ar atmosphere	[27]
CuCl_2 molten salt	$\text{Ti}_3\text{SiC}_2/\text{Ti}_3\text{C}_2\text{T}_x$	@ 750 °C; Can etch Si, Ga and Zn ‘A’ layers.	[28]

and even high concentration alkali solutions (as an HF-free option) are also proven to be successful etchants [23–25]. However, time, temperature, concentration and other etching conditions differ a lot for various MAX phases and individual optimization is required for every case. In general, by increasing the atomic number of the transition metal and/or ‘n’ (in M_{n+1}X_n), longer etching times and stronger etchants are needed [10].

The product of etching is called multilayered MXene (m-MXene) which has 2–6 times stronger interlayer attractions than graphene and other 2D materials [29]. Hence, even after successful removal of the ‘A’ layer, it is very difficult to delaminate the m-MXene to single layers. Consequently, an additional intercalation step is required to further increase the interlayer spacing and facilitate the delamination process [8]. Polar solvents (e.g. DMSO), hydrazine, urea [30] and even large organic base molecules (e.g. tetrabutylammonium hydroxide or n-butylamine) [12] have been effectively used as intercalation agents. Metal cations are also efficient intercalants since MXene sheets have a substantial amount of negative surface charges (due to the functional groups) [31]. Accordingly, when etching with the ‘strong acid and fluoride salt’ technique, also known as minimally intensive layer delamination (MILD), metallic cations of the salt (e.g. Li^+ in the case of $\text{LiF} + \text{HCl}$) serve as the intercalating agent [10]. After the intercalation step, delaminated MXene (d-MXene) can be obtained by a vigorous mechanical agitation or an ultrasonic treatment process. In general, mechanical agitation yields a higher quality product with larger flake size and lower defect level [32]. It is noteworthy that MXenes are prone to oxidation, especially in aqueous suspensions and in presence of oxygen [33]. Hence, MXene inks with organic anhydrous carrier solvents are chemically more stable than their aqueous counterparts, however, at the cost of electronic conductivity measured from the four-point probe of MXene films. Through deoxygenation and storing of the delaminated dispersion in hermetic argon-filled vessels at low temperatures (e.g. 5 °C), the shelf-life of MXene inks can be substantially extended. It has been also found that inks with higher concentration show better oxidation resistance than dilute inks [34].

3. MXene inks for printed/coated EESDs

The rheological properties of MXene inks, as a determining factor for their processability, highly depend on their concentration. Other parameters such as particle size distribution, nanosheets aspect ratio, and degree of functionalization can also affect the rheological properties and should be considered while formulating inks. In general, by varying the concentration of the MXene inks (low, medium, and high), three distinct regimes in their rheological behavior can be observed. For instance, for a m-MXene dispersion with a

medium particle size of 5 μm , at low concentrations (e.g. 10 wt.%), particles are randomly dispersed with little interactions with each other, while at medium concentrations (e.g. 30 wt.%) a sol-gel transition (viscous at low frequencies and gel at high frequencies) can be observed. At high concentrations (>40 wt.%), the percolated network of nanosheets forms a colloidal gel with a considerable yield strength [13]. Each of these behavioral regimes can be used (by simply adjusting the solid content) for formulation of inks for various liquid-phase techniques, from spray- and spin-coating to screen- and extrusion-printing. The appropriate printing or coating technique and consequently the proper ink for fabrication of an EESD is selected by considering its application. While in most applications, deposition of thick films is highly desirable, in some specific cases, formation of thin films is a must. In the following sections, some of the recent examples of the formulated MXene inks for different types of EESDs and major printing/coating techniques with their required rheological properties have been reviewed.

3.1. Low-concentration inks

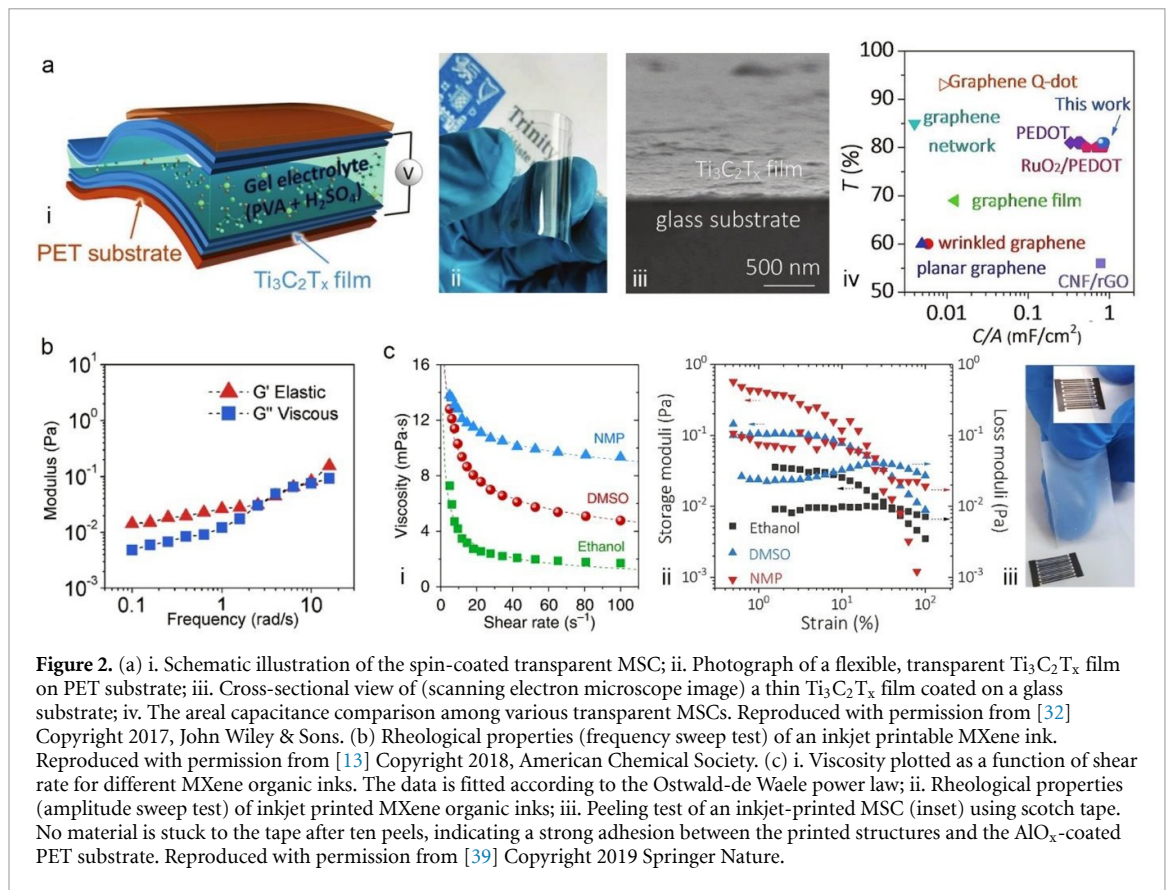
One of the main applications of low-concentration inks are thin films for the fabrication of transparent devices. This is mainly due to the fact that the transmittance decays exponentially with the thickness of the films. However, in low-concentration viscoelastic suspensions, the viscous characteristics are usually dominant, and the elastic properties are negligible. Nevertheless, the spin- or spray-coating techniques which are the most used methods for liquid-phase deposition of thin films, require a specific level of elastic behavior for elimination of the process-imposed perturbations [35]. MXene inks, even at low concentrations ($<0.36 \text{ mg.ml}^{-1}$), exhibit surprisingly high levels of elastic behavior [13], which allow the realization of transparent films with both spray- and spin-coating methods [32, 36]. In addition to their suitable rheological properties, MXenes are a unique choice for fabrication of transparent EESDs owing to their exceptional electrochemical properties. Indeed, the number of choices for transparent liquid-phase-processable materials are limited to conductive metal oxides, carbon nanotubes, graphenes (pristine and functionalized), MXenes, metallic nanowires (e.g. Ag NWs), and conducting polymers [37, 38]. Amongst all, for a specific optical transmittance (e.g. >90%) in the visible range, MXenes are the only group which simultaneously offer high conductivity and charge storage capacitance [32]. In this regard, Zhang *et al* have reported a spin-coated, flexible, transparent (72% transmission) $\text{Ti}_3\text{C}_2\text{T}_x$ supercapacitor with impressive areal (0.48 mF.cm^{-2}) and volumetric (676 F.cm^{-3}) capacitances (figure 2(a)). Such high figures of merit have only become possible thanks to the utilization of a MILD technique for etching and a handshake-agitation for a gentle delamination which has resulted in high quality large flakes with a very low percolation threshold [32].

Formulation of ink for some specific printing techniques is another case where low-concentration suspensions are needed. For instance, inkjet printing (IJP) which is a digital non-contact printing method can only handle low-viscosity inks ($<10 \text{ cP}$). An IJP ink, in addition to specific surface tension and viscosity, should show viscous behavior at the jetting step and quick recovery of elastic properties after deposition, to avoid uncontrolled spreading of droplets [35]. This behavior is reflected in domination of the storage modulus (G') at low frequencies (long-range interactions) and the loss modulus (G'') at mid to high frequencies (short-range interactions) in a frequency sweep test (figure 2(b)) [13]. Despite the fact that MXenes are usually synthesized in water and disperse in it better than in any other solvent; due to the high surface tension of additive-free aqueous inks (poor jetting/wetting), it is necessary to formulate inks in alternative solvents.

Recently, Zhang *et al* have prepared MXene ($\text{Ti}_3\text{C}_2\text{T}_x$) IJP inks in various polar solvents through sonicating the multilayered MXene in various organic solvents [39]. While all formulated inks possess viscosities in the processing range of IJP, they all exhibit yield stress which can be attributed to the crowding of particles and consequently gelation of the system as a result of the repulsive interactions experienced by neighboring MXene sheets [35] (figure 2(c)). Micro-supercapacitors (MSCs) with an interdigitated structure (gap size: $89 \mu\text{m}$) have been printed on Al_2O_3 coated PET substrates and a remarkable volumetric capacitance of 562 F.cm^{-3} has been obtained. It is noteworthy that the performance of the printed MSCs were different for each formulation, and NMP-based ink (N-Methyl-2-pyrrolidone; 12.5 mg.ml^{-1}) yielded the best results. Even though that no binder was used in ink formulation, the printed traces showed exceptional mechanical integrity and adhesion (to the substrate), mainly because of the strong interactions of the functional groups.

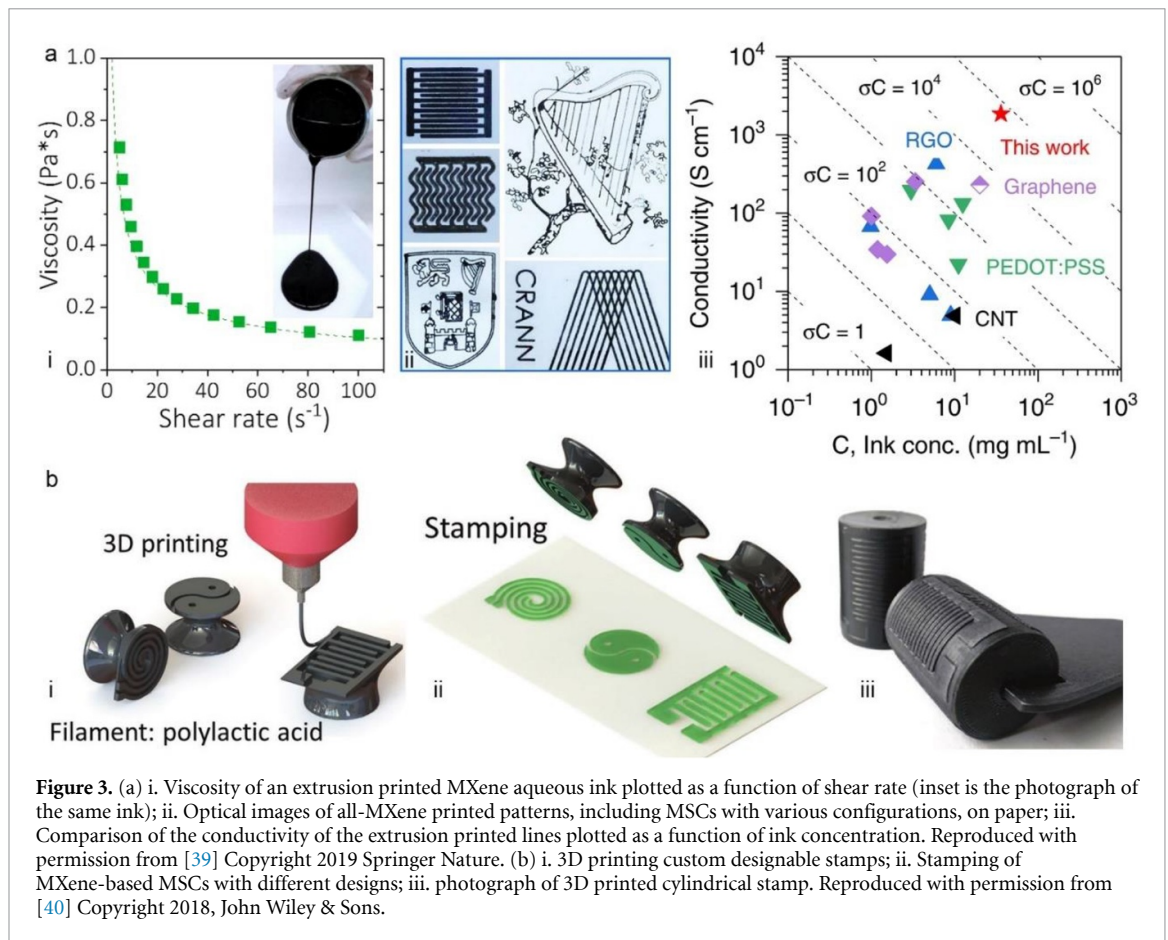
3.2. Medium- or high-concentration inks

As mentioned earlier, in majority of the applications, high-concentration inks are preferable for fabrication of EESDs since more materials can be deposited during each printing/coating pass. This is because of the fact that the total stored charge in an EESD is directly related to the active surface area and the amount of the electrochemically active material. Increasing the solid content of inks upsurge their viscosity and necessitates the use of printing/coating techniques designed for high viscosity liquids. An ideal ink for an efficient



printing, in addition to a high concentration (c) should also possess a high electronic conductivity (σ) [39]. To evaluate the electronic properties of an ink, a figure of merit which takes both of these properties into account ($\text{FoM} = \sigma c [\text{S} \cdot \text{cm}^{-1} \cdot \text{mg} \cdot \text{ml}^{-1}]$) is typically used, and its higher values correspond to better inks. For instance, an aqueous $\text{Ti}_3\text{C}_2\text{T}_x$ MXene ink ($36 \text{ mg} \cdot \text{ml}^{-1}$) formulated by Zhang *et al* for 2D extrusion printing of MSCs on a paper substrate has shown a record-high FoM of $66\,996 \text{ S} \cdot \text{cm}^{-1} \cdot \text{mg} \cdot \text{ml}^{-1}$ [39] which is ~ 11 fold higher than the best reported graphene ink ($6000 \text{ S} \cdot \text{cm}^{-1} \cdot \text{mg} \cdot \text{ml}^{-1}$) [2]. The MSCs printed with this ink (figure 3(a)) have showcased energy densities as high as $0.32 \mu\text{W} \cdot \text{h} \cdot \text{cm}^{-2}$ at a power density of $11.4 \mu\text{W} \cdot \text{cm}^{-2}$, and a 3-pass, extrusion printed device has exhibited higher areal capacitance than its 25-pass inkjet-printed counterpart ($12.5 \text{ mg} \cdot \text{ml}^{-1}$ $\text{Ti}_3\text{C}_2\text{T}_x$ MXene in NMP ink). Zhang *et al* has also developed two other aqueous inks ($\text{Ti}_3\text{C}_2\text{T}_x$ and Ti_3CNT_x) with similar rheological properties for a customizable stamping technique [40]. Flat and cylindrical stamps, capable of performing the material transfer processes used in sheet-to-roll and roll-to-roll methods, have been printed by a 3D printer with various patterns (figure 3(b)). Printed MSCs delivered areal capacitances as high as $61 \text{ mF} \cdot \text{cm}^{-2}$ at $25 \mu\text{A} \cdot \text{cm}^{-2}$, demonstrating promising scale-up possibilities. Indeed, owing to their enormous production yield, both techniques are extremely appealing for commercialization of MXene-based EESDs.

To further increase the areal power and energy densities, inks with much higher solid contents ($>20 \text{ wt.}\%$) are required. This leads to a dramatic increase in the viscosity of the inks which limits the application methods to screen- and 3D-printing techniques. Recently by Zhang and colleagues [41], a novel aqueous $\text{Ti}_3\text{C}_2\text{T}_x$ ink with 22 wt.% solid content, mostly based on m-MXene and unetched MAX phase, has been formulated for scalable screen-printing of MSCs (figure 4(a)). With a lower degree of exfoliation, solid content can be boost up without dramatically increasing the viscosity [13]. Replacing the d-MXene with m-MXene in ink formulation is vital as production of a d-MXene ink with the same concentration is difficult and its ultra-high viscosity renders it unprocessable even with the screen-printing method. The exceptionally high areal capacitance and energy density of the printed MSCs ($158 \text{ mF} \cdot \text{cm}^{-2}$ and $1.64 \mu\text{W} \cdot \text{h} \cdot \text{cm}^{-2}$, respectively) confirms that after a printing and drying step, the active surface area for both d- and m-MXene are comparable. It has also been found that addition of a small amount of d-MXene ($\sim 2\%$) to the formulated inks is crucial for obtaining decent mechanical properties in the printed structures. Considering the low synthesis yield of d-MXene (10%–20%), application of m-MXene and unetched MAX phase which are typically trashed away during the synthesis of d-MXene, can considerably reduce the fabrication costs and pave the road towards commercial printing of MXene-based EESDs.



The effect of the flake size and aspect ratio on the rheological properties of the MXene inks has also been highlighted by Yang *et al* [42]. They have formulated an additive-free extrusion printing ink with ultrahigh aspect ratio (~ 4000) flakes which has exhibited viscosity values in the same order of magnitude as another reported ink with three orders of magnitude higher concentration. A mild etching technique (without the ultrasonic treatment) has been used to obtain such high aspect ratio flakes. Inks with various concentrations have been formulated and all of them have shown little thixotropy and high yield strength which is necessary for 3D printing methods (figure 4(b)). By freeze drying the printed MSCs, highly porous 3D interdigitated structures (finger diameter of $326\ \mu\text{m}$ and gap distance of $187\ \mu\text{m}$) with an areal capacitance as high as $2.1\ \text{F}\cdot\text{cm}^{-2}$ at $1.7\ \text{mA}\cdot\text{cm}^{-2}$ and superior energy and power densities (e.g. $0.0244\ \text{mWh}\cdot\text{cm}^{-2}$ at $0.64\ \text{mW}\cdot\text{cm}^{-2}$) are realized.

Due to the strong electrostatic repulsions of MXene nanosheets, conventional techniques for increasing the concentration of the colloidal suspensions (e.g. centrifugation) are not applicable. High-temperature evaporation is also not an option since MXene are extremely prone to oxidation under such conditions. In an attempt to formulate additive-free 3D-printable MXene ink, Beidaghi *et al* [43] have used superabsorbent polymer beads to remove the excess water from their synthesized $\text{Ti}_3\text{C}_2\text{T}_x$ MXene suspension and increase the concentration from $10\ \text{mg}\cdot\text{mL}^{-1}$ to $290\ \text{mg}\cdot\text{mL}^{-1}$. A 3D printable ink should exhibit a shear thinning behavior with a certain minimum yield stress (depends on the printer). The viscoelastic properties of the formulated inks should be accurately adjusted to ensure proper shape retention and interlayer adhesion in printed structures. The storage to loss modulus ratio (G'/G'') is a useful measure for evaluating the 3D-printability of an ink, where a value between $2 < G'/G'' < 20$ is highly desirable (figure 4(c)). The 3D printed, highly flexible MSCs have showcased impressive areal capacitance of $1035\ \text{mF}\cdot\text{cm}^{-2}$ at $2\ \text{mV}\cdot\text{s}^{-1}$ and energy density of $51.7\ \mu\text{W}\cdot\text{h}\cdot\text{cm}^{-2}$. Yu *et al* have demonstrated another big advantage of the MXene-based inks by formulating screen- and extrusion-printing inks using nitrogen-doped crumpled $\text{Ti}_3\text{C}_2\text{T}_x$ sheets [44]. Even in this case, the formulated additive-free inks maintain the proper rheological properties and film formation behavior of the pure MXenes. This is an important finding since it adds another level of freedom to ink formulation strategies and enables realization of high porosity structures. By opting for such an approach, MSCs with high areal capacitance (screen printed; $70.1\ \text{mF}\cdot\text{cm}^{-2}$) as well as high areal and volumetric energy densities (extrusion printed; $0.42\ \text{mWh}\cdot\text{cm}^{-2}$ and $0.83\ \text{mWh}\cdot\text{cm}^{-3}$, respectively) have been fabricated. The summary of the reviewed printed/coated MSCs is provided in table 2.

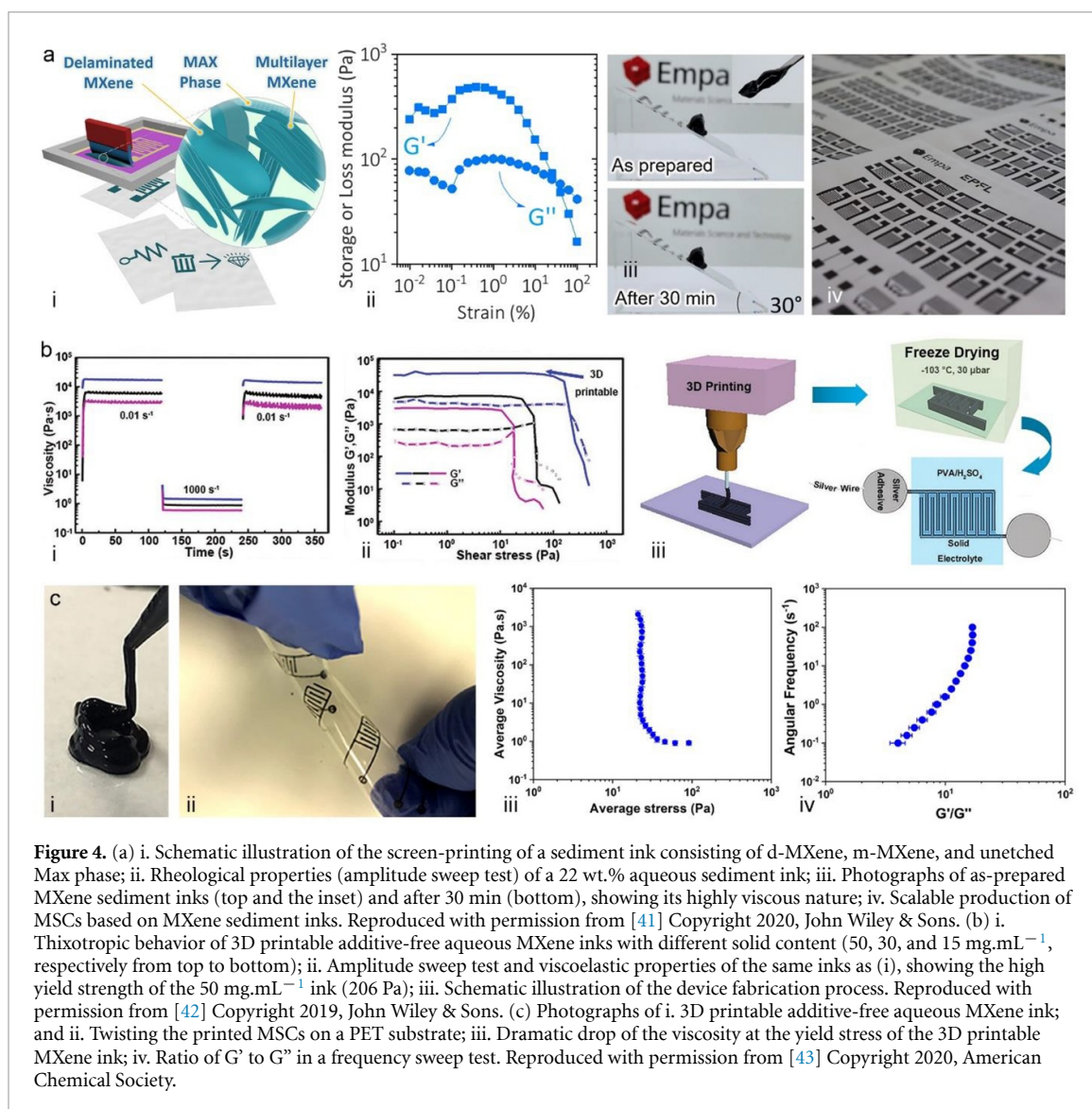
Table 2. Summary of the reviewed printed/coated MSCs.

Printing/Coating method	Ink composition	Electrochemical performance	Potential window	Ref. #
Spin coating	Ti ₃ C ₂ T _x /water 1.5 mg.mL ⁻¹	Areal capacitance: 0.48 mF.cm ⁻² Volumetric capacitance: 676 F.cm ⁻³	0.65 V	[32]
Inkjet printing	Ti ₃ C ₂ T _x /NMP 12 mg.mL ⁻¹	Volumetric capacitance: 562 F.cm ⁻³	0.5 V	[39]
2D Extrusion printing	Ti ₃ C ₂ T _x /water 36 mg.mL ⁻¹	Energy density: 0.32 μ W.h.cm ⁻² at a power density of 11.4 μ W.cm ⁻²	0.5 V	[39]
Transfer printing (stamp)	Ti ₃ C ₂ T _x /water 22 mg.mL ⁻¹ Ti ₃ CNT _x /water 24 mg.mL ⁻¹	Areal capacitance: 61 mF.cm ⁻² at 25 μ A.cm ⁻²	0.6 V	[40]
Screen printing	m-Ti ₃ C ₂ T _x /water 22 wt. %	Areal capacitance: 158 mF.cm ⁻² Energy density: 1.64 μ Wh.cm ⁻²	0.6 V	[41]
Screen printing	N-Ti ₃ C ₂ T _x /CB/LA132- binder/water wt. ratio: 8:1:1:13.6 34 wt. %	Areal capacitance: 70.1 mF.cm ⁻²	0.6 V	[44]
3D Extrusion printing	CNT/AC/N-Ti ₃ C ₂ T _x /GO wt. ratio: 1:3:3:1	Areal energy density: 0.42 mWh.cm ⁻² Vol. energy dens- ity: 0.83 mWh.cm ⁻³	0.6 V	[44]
3D Extrusion printing	Ti ₃ C ₂ T _x /water 50 mg.mL ⁻¹	Areal capacitance: 2.1 F.cm ⁻² at 1.7 mA.cm ⁻² Energy density: 0.0244 mWh.cm ⁻² at Power density: 0.64 mW.cm ⁻²	0.6 V	[42]
3D Extrusion printing	Ti ₃ C ₂ T _x /water 290 mg.mL ⁻¹	Areal capacitance: 1035 mF.cm ⁻² at 2 mV.s ⁻¹ Energy density: 51.7 μ W.h.cm ⁻²	0.6 V	[43]

3.3. MXene as a functional additive

In all the afore-reviewed works, MXenes have been used as the electrochemically active component of the inks; nevertheless, they can also be used as a functional additives [1, 45]. Unlike conventional additives (e.g. polymeric binders) which usually have adverse effects on the functionality of the printed/coated structures, functional additives improve the performance of the devices. For instance, in fabrication of Li-ion battery anodes, since silicon nanoparticles (Si NPs) themselves are not coatable, a polymeric binder which is usually an insulator material is inevitable in the battery electrodes. To ensure the charge transport throughout the electrode, a conductive agent should also be added to boost the electrical conductivity. The conductive agents usually form a point-to-point type of connection with the Si NPs which can be easily lost upon repeated volume expansions/contractions of charge/discharge cycles (figure 5(a)). Zhang and co-workers have addressed this mechanical instability by replacing the conventional dual-component additives (PAA/carbon black, CB) from anode fabrication inks with MXenes (Ti₃C₂T_x and Ti₃CNT_x) [46]. Since MXenes establish a point-to-plane type of contact with Si NPs, the volumetric fluctuations can be well accommodated, and a proper connection can be maintained. They have also found that MXene-based inks possess much higher viscosities (orders of magnitude) than their PAA-based counterparts with a similar solid content. This is a very important finding since the critical cracking thickness (CCT) of a film is determined by the viscosity and surface tension of the slurry [47]. Based on this fact, they are able to increase the CCT of their films from < 100 μ m (for PAA-based ink) to ~350 μ m (for MXene-based ink). As a result, extremely high areal capacity anodes (up to 23.3 mA.h.cm⁻²) with significantly higher conductivity (increased by 1200 times) and tensile toughness (increased by 40 times) have been realized. It is noteworthy that the adhesion of the films to the copper current collector was high enough to eliminate the need of a binder for that purpose as well.

The functionality of MXenes as an ink additive can be even multiplied by functionalization or decoration with specific particles. Sulfur is one of such materials which despite its high theoretical energy density (2570 W.h.kg⁻¹) as a cathode for Li-S batteries, had limited success, mainly because of its insulating nature and notorious shuttling effect of intermediate lithium polysulfides (Li₂S_x, x > 3) [48]. Carbonaceous additives, due to their non-polar nature, cannot provide a proper confinement for polar Li₂S_x [49]. In contrast, the abundant electronegative surface groups of MXenes (such as -O and -OH) can effectively



anchor S NPs via electrostatic interactions. Based on this fact, Zhang *et al* have formulated a highly viscous aqueous MXene (Ti₃C₂T_x) ink decorated with S for slurry casting (figure 5(b)) [50]. The ink exhibits a shear-thinning (pseudoplastic) behavior which follows the Ostwald-de Waele power law ($\eta \propto k\dot{\gamma}^{n-1}$, $n = 0.21$). The high concentration and viscosity (≈ 20 mg.mL⁻¹ and 12.4 Pa.s, respectively) have enabled the ink to be arbitrarily coated on various substrates such as Celgard membranes, paper, aluminum foil and stainless steel without the need for any other additive. Extremely high capacity (up to 1350 mA.h.g⁻¹), excellent rate handling, and ultralow capacity decay rate (as low as 0.035% per cycle, after 175 cycles) were reported. The impressive electrochemical performance are attributed to the synergistic effects between S NPs and conductive, polar Ti₃C₂T_x backbone, where the electron transport and ion diffusion kinetics have been substantially enhanced.

4. Conclusions and perspectives

In summary, we reviewed the major printing and coating techniques for fabrication of MXene-based EESDs, as well as ink formulation strategies, rheological requirements and processability considerations of each method. The unique properties of MXenes rendering them an ideal choice for liquid-phase fabrication of EESDs are also discussed. While great progresses in synthesis of MXenes and their ink formulations have been made, some additional investigations and further improvements are still required to witness the commercial printing and coating of MXene-based EESDs. The following aspects, we believe, are current challenges and future perspectives in processing of MXenes that should be highlighted.

Regarding the synthesis step, improving the delamination and etching yields is necessary for lowering the overall production costs. Most of the available synthesis recipes are optimized for few grams of MAX phase

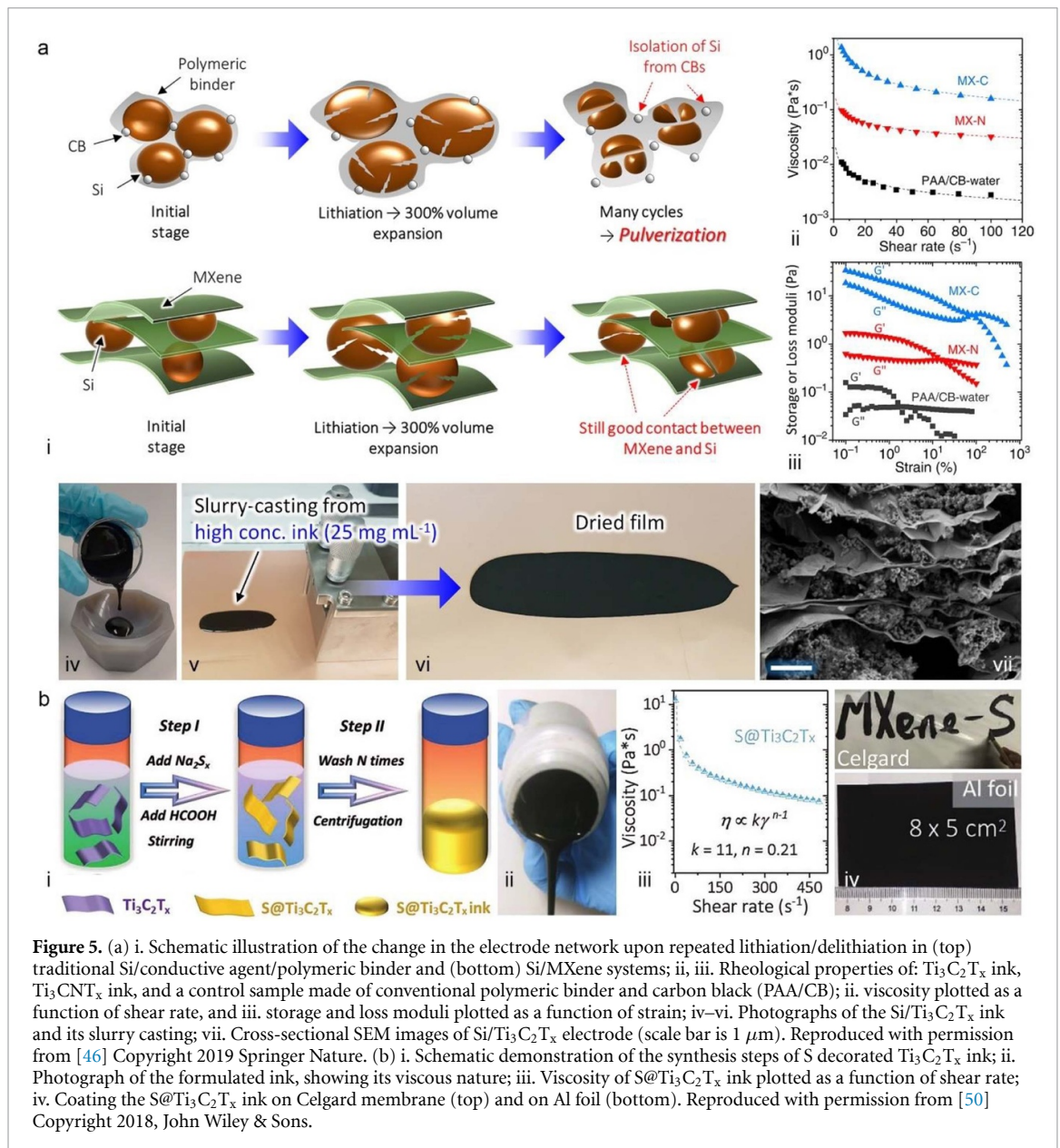


Figure 5. (a) i. Schematic illustration of the change in the electrode network upon repeated lithiation/delithiation in (top) traditional Si/conductive agent/polymeric binder and (bottom) Si/MXene systems; ii, iii. Rheological properties of: $\text{Ti}_3\text{C}_2\text{T}_x$ ink, Ti_3CNT_x ink, and a control sample made of conventional polymeric binder and carbon black (PAA/CB); ii. viscosity plotted as a function of shear rate, and iii. storage and loss moduli plotted as a function of strain; iv–vi. Photographs of the Si/ $\text{Ti}_3\text{C}_2\text{T}_x$ ink and its slurry casting; vii. Cross-sectional SEM images of Si/ $\text{Ti}_3\text{C}_2\text{T}_x$ electrode (scale bar is $1 \mu\text{m}$). Reproduced with permission from [46] Copyright 2019 Springer Nature. (b) i. Schematic demonstration of the synthesis steps of S decorated $\text{Ti}_3\text{C}_2\text{T}_x$ ink; ii. Photograph of the formulated ink, showing its viscous nature; iii. Viscosity of $\text{S}@\text{Ti}_3\text{C}_2\text{T}_x$ ink plotted as a function of shear rate; iv. Coating the $\text{S}@\text{Ti}_3\text{C}_2\text{T}_x$ ink on Celgard membrane (top) and on Al foil (bottom). Reproduced with permission from [50] Copyright 2018, John Wiley & Sons.

while the majority of the printing and coating methods require several hundred grams of ink. Since the type and concentration of the terminal groups, density of defects, and size of flakes are strongly dependent on the synthesis method and process conditions, upscaling the synthesis of MXenes is a big challenge. Current MXene synthesis methods have little or no control on the type and uniformity of the terminal groups while their role on the rheological properties, film formation and device performance are very well documented. Thus, development of large-scale synthesis methods with proper control on the terminal groups and capable of delivering products with consistent quality would be one of the main research topics.

Considering the ink formulation, especially non-aqueous inks and their rheological properties and film formation behavior, there exists a big knowledge gap. Currently available literature has also only focused on $\text{Ti}_3\text{C}_2\text{T}_x$ MXene with random functional groups. The effect of specific terminal groups on rheological properties, film formation, and device performance has not been fully understood. The relatively short shelf-life of the MXene inks (compared to graphene or metallic inks) is another issue which requires further attention. Printed/coated MXene films and structures have better oxidation resistance after complete evaporation of the solvent but further improvements are needed specially for the devices which are exposed to the environmental conditions (such as oxygen and humidity). Pre- and post-treatments can potentially improve the chemical stability of the MXenes. While recently some promising reports have been published [51, 52], there is still a huge need for further investigations.

From the ‘electrochemical performance’ point of view, even though MXenes are viewed as the next-generation energy storage materials, there are still important challenges to be addressed, some of which are mentioned here:

- Small voltage window in aqueous electrolytes (~ 0.6 V in the symmetric devices);
- Potential instability of the electrodes (if immersed in the flooded cell);
- Capacitance and charge storage properties still need to be further improved.

While numerous solutions are conceivable for these challenges, some of the most promising approaches can be summarized as:

- Heteroatom(s) doping of the MXene skeleton, or fabrication of asymmetric devices (pairing with a more positive electrode) for widening the voltage window;
- Constructing (semi-) solid-state supercapacitor devices to solve the potential instability of MXene electrodes. Since the water content is greatly reduced, the films can maintain their compact morphology without being attacked by the water molecules and dissolved oxygen;
- Introducing heteroatoms (such as doping nitrogen, sulfur, phosphorus, boron, etc.) or heterostructures to the MXene framework (e.g. with MoS_2 , MoSe_2 , etc.) to enhance the capacitance as well as rate performance. In addition, engineering the defects chemistry (such as location and density) and surface chemistry (i.e. type, amount, and relative ratio of the functional groups) are also expected to be efficient.

The possibility of formulating aqueous inks from MXenes opens up the perspective for green and environmental-friendly manufacturing of devices. Furthermore, methods for surface functionalization and/or the formation of MXene composites are only in the early stages, with many novel device possibilities to be expected.

Acknowledgments

The authors acknowledge funding from an Empa internal research grant. Financial support from the project FOXIP in the framework of the Strategic Focus Area (SFA) Advanced Manufacturing of the ETH Board is acknowledged.

ORCID iDs

Sina Abdolhosseinzadeh  <https://orcid.org/0000-0002-3536-2541>

Chuanfang (John) Zhang  <https://orcid.org/0000-0001-8663-3674>

References

- [1] Hu G, Kang J, Ng I W T, Zhu X, Howe R C T, Jones C G, Hersam M C and Hasan T 2018 Functional inks and printing of two-dimensional materials *Chem. Soc. Rev.* **47** 3265–300
- [2] Secor E B, Ahn B Y, Gao T Z, Lewis J A and Hersam M C 2015 Rapid and versatile photonic annealing of graphene inks for flexible printed electronics *Adv. Mater.* **27** 6683–8
- [3] Schneider M, Koos E and Willenbacher N 2016 Highly conductive, printable pastes from capillary suspensions *Sci. Rep.* **6** 1–10
- [4] Naguib M, Kurtoglu M, Presser V, Lu J, Niu J, Heon M, Hultman L, Gogotsi Y and Barsoum M W 2011 Two-dimensional nanocrystals produced by exfoliation of Ti_3AlC_2 *Adv. Mater.* **23** 4248–53
- [5] Wang G *et al* 2020 Two-photon absorption in monolayer MXenes *Adv. Opt. Mater.* **8** 1902021
- [6] Yun T *et al* 2020 Electromagnetic shielding of monolayer MXene assemblies *Adv. Mater.* **32** 1906769
- [7] Lyu B, Kim M, Jing H, Kang J, Qian C, Lee S and Cho J H 2019 Large-area MXene electrode array for flexible electronics *ACS Nano* **13** 11392–400
- [8] Anasori B, Lukatskaya M R and Gogotsi Y 2017 2D metal carbides and nitrides (MXenes) for energy storage *Nat. Rev. Mater.* **2** 16098
- [9] Anasori B, Xie Y, Beidaghi M, Lu J, Hosler B C, Hultman L, Kent P R C, Gogotsi Y and Barsoum M W 2015 Two-dimensional, ordered, double transition metals carbides (MXenes) *ACS Nano* **9** 9507–16
- [10] Zhang C (John), Ma Y, Zhang X, Abdolhosseinzadeh S, Sheng H, Lan W, Pakdel A, Heier J and Nüesch F 2020 Two-dimensional transition metal carbides and nitrides (MXenes): synthesis, properties, and electrochemical energy storage applications *Energy Environ. Mater.* **3** 29–55
- [11] Abdolhosseinzadeh S, Sadighikia S and Alkan Gürsel S 2018 Scalable synthesis of sub-nanosized platinum-reduced graphene oxide composite by an ultraprecise photocatalytic method *ACS Sustain. Chem. Eng.* **6** 3773–82
- [12] Naguib M, Unocic R R, Armstrong B L and Nanda J 2015 Large-scale delamination of multi-layers transition metal carbides and carbonitrides “MXenes” *Dalton Trans.* **44** 9353–8
- [13] Akuzum B, Maleski K, Anasori B, Lelyukh P, Alvarez N J, Kumbur E C and Gogotsi Y 2018 Rheological characteristics of 2D titanium carbide (MXene) dispersions: a guide for processing MXenes *ACS Nano* **12** 2685–94

- [14] Dong Y, Shi H and Wu Z 2020 Recent advances and promise of MXene-based nanostructures for high-performance metal ion batteries *Adv. Funct. Mater.* **2000706**
- [15] Garg R, Agarwal A and Agarwal M 2020 A review on MXene for energy storage application: effect of interlayer distance *Mater. Res. Express* **7** 22001
- [16] Tontini G, Greaves M, Ghosh S, Bayram V and Barg S 2020 MXene-based 3D porous macrostructures for electrochemical energy storage *J. Phys.: Mater.* **3** 22001
- [17] Abdolhosseinzadeh S, Asgharzadeh H and Kim H S 2015 Fast and fully-scalable synthesis of reduced graphene oxide *Sci. Rep.* **5** 10160
- [18] Zhou J, Zha X, Chen F Y, Ye Q, Eklund P, Du S and Huang Q 2016 A two-dimensional zirconium carbide by selective etching of Al_3C_3 from Nanolaminated $\text{Zr}_3\text{Al}_3\text{C}_5$ *Angew. Chem. Int. Ed.* **55** 5008–13
- [19] Wang H W, Naguib M, Page K, Wesolowski D J and Gogotsi Y 2016 Resolving the structure of $\text{Ti}_3\text{C}_2\text{T}_x$ MXenes through multilevel structural modeling of the atomic pair distribution function *Chem. Mater.* **28** 349–59
- [20] Halim J, Cook K M, Naguib M, Eklund P, Gogotsi Y, Rosen J and Barsoum M W 2016 X-ray photoelectron spectroscopy of select multi-layered transition metal carbides (MXenes) *Appl. Surf. Sci.* **362** 406–17
- [21] Hope M A, Forse A C, Griffith K J, Lukatskaya M R, Ghidui M, Gogotsi Y and Grey C P 2016 NMR reveals the surface functionalisation of Ti_3C_2 MXene *Phys. Chem. Chem. Phys.* **18** 5099–102
- [22] Ghidui M, Lukatskaya M R, Zhao M-Q, Gogotsi Y and Barsoum M W 2014 Conductive two-dimensional titanium carbide ‘clay’ with high volumetric capacitance *Nature* **516** 78–81
- [23] Feng A, Yu Y, Jiang F, Wang Y, Mi L, Yu Y and Song L 2017 Fabrication and thermal stability of NH_4HF_2 -etched Ti_3C_2 MXene *Ceram. Int.* **43** 6322–8
- [24] Wang L, Zhang H, Wang B, Shen C, Zhang C, Hu Q, Zhou A and Liu B 2016 Synthesis and electrochemical performance of $\text{Ti}_3\text{C}_2\text{T}_x$ with hydrothermal process *Electron. Mater. Lett.* **12** 702–10
- [25] Li T et al 2018 Fluorine-Free Synthesis of High-Purity $\text{Ti}_3\text{C}_2\text{T}_x$ ($\text{T}=\text{OH}, \text{O}$) via Alkali Treatment *Angew. Chem. Int. Ed.* **57** 6115–9
- [26] Wu J, Wang Y, Zhang Y, Meng H, Xu Y, Han Y, Wang Z, Dong Y and Zhang X 2020 Highly safe and ionothermal synthesis of Ti_3C_2 MXene with expanded interlayer spacing for enhanced lithium storage *J. Energy Chem.* **47** 203–9
- [27] Urbankowski P, Anasori B, Makaryan T, Er D, Kota S, Walsh P L, Zhao M, Shenoy V B, Barsoum M W and Gogotsi Y 2016 Synthesis of two-dimensional titanium nitride Ti_4N_3 (MXene) *Nanoscale* **8** 11385–91
- [28] Li Y et al 2020 A general Lewis acidic etching route for preparing MXenes with enhanced electrochemical performance in non-aqueous electrolyte *Nat. Mater.* **19** 894–9
- [29] Hu T, Hu M, Li Z, Zhang H, Zhang C, Wang J and Wang X 2016 Interlayer coupling in two-dimensional titanium carbide MXenes *Phys. Chem. Chem. Phys.* **18** 20256–60
- [30] Mashtalir O, Naguib M, Mochalin V N, Dall’Agnese Y, Heon M, Barsoum M W and Gogotsi Y 2013 Intercalation and delamination of layered carbides and carbonitrides *Nat. Commun.* **4** 1–7
- [31] Osti N C et al 2016 Effect of metal ion intercalation on the structure of MXene and water dynamics on its internal surfaces *ACS Appl. Mater. Interfaces* **8** 8859–63
- [32] Zhang C J, Anasori B, Seral-Ascaso A, Park S-H, McEvoy N, Shmeliov A, Duesberg G S, Coleman J N, Gogotsi Y and Nicolosi V 2017 Transparent, flexible, and conductive 2D titanium carbide (MXene) films with high volumetric capacitance *Adv. Mater.* **29** 1702678
- [33] Chae Y, Kim S J, Cho S Y, Choi J, Maleski K, Lee B J, Jung H T, Gogotsi Y, Lee Y and Ahn C W 2019 An investigation into the factors governing the oxidation of two-dimensional Ti_3C_2 MXene *Nanoscale* **11** 8387–93
- [34] Zhang C J et al 2017 Oxidation stability of colloidal two-dimensional titanium carbides (MXenes) *Chem. Mater.* **29** 4848–56
- [35] Naficy S, Jalili R, Aboutalebi S H, Gorkin R A, Konstantinov K, Innis P C, Spinks G M, Poulin P and Wallace G G 2014 Graphene oxide dispersions: tuning rheology to enable fabrication *Mater. Horiz.* **1** 326–31
- [36] Hantanasirisakul K, Zhao M-Q, Urbankowski P, Halim J, Anasori B, Kota S, Ren C E, Barsoum M W and Gogotsi Y 2016 Fabrication of $\text{Ti}_3\text{C}_2\text{T}_x$ MXene transparent thin films with tunable optoelectronic properties *Adv. Electron. Mater.* **2** 1600050
- [37] Zhang C (John) and Nicolosi V 2019 Graphene and MXene-based transparent conductive electrodes and supercapacitors *Energy Storage Mater.* **16** 102–25
- [38] Zhang C (John), Higgins T M, Park S H, O’Brien S E, Long D, Coleman J N and Nicolosi V 2016 Highly flexible and transparent solid-state supercapacitors based on RuO_2 /PEDOT:PSS conductive ultrathin films *Nano Energy* **28** 495–505
- [39] Zhang C (John) et al 2019 Additive-free MXene inks and direct printing of micro-supercapacitors *Nat. Commun.* **10** 1795
- [40] Zhang C J, Kremer M P, Seral-Ascaso A, Park S-H, McEvoy N, Anasori B, Gogotsi Y and Nicolosi V 2018 Stamping of flexible, coplanar micro-supercapacitors using MXene inks *Adv. Funct. Mater.* **28** 1705506
- [41] Abdolhosseinzadeh S, Schneider R, Verma A, Heier J, Nüesch F and Zhang C 2020 Turning trash into treasure: additive free MXene sediment inks for screen-printed micro-supercapacitors *Adv. Mater.* **32** 2000716
- [42] Yang W, Yang J, Byun J J, Moissinac F P, Xu J, Haigh S J, Domingos M, Bissett M A, Dryfe R A W and Barg S 2019 3D printing of freestanding MXene architectures for current-collector-free supercapacitors *Adv. Mater.* **31** 1902725
- [43] Orangi J, Hamade F, Davis V A and Beidaghi M 2020 3D printing of additive-free 2D $\text{Ti}_3\text{C}_2\text{T}_x$ (MXene) ink for fabrication of micro-supercapacitors with ultra-high energy densities *ACS Nano* **14** 640–50
- [44] Yu L, Fan Z, Shao Y, Tian Z, Sun J and Liu Z 2019 Versatile N-doped MXene ink for printed electrochemical energy storage application *Adv. Energy Mater.* **9** 1901839
- [45] Zhang C (John), Cui L, Abdolhosseinzadeh S and Heier J 2020 Two-dimensional MXenes for lithium-sulfur batteries *InfoMat* **2** 613–38
- [46] Zhang C (John), Park S H, Seral-Ascaso A, Barwich S, McEvoy N, Boland C S, Coleman J N, Gogotsi Y and Nicolosi V 2019 High capacity silicon anodes enabled by MXene viscous aqueous ink *Nat. Commun.* **10** 849
- [47] Du Z, Rollag K M, Li J, An S J, Wood M, Sheng Y, Mukherjee P P, Daniel C and Wood D L 2017 Enabling aqueous processing for crack-free thick electrodes *J. Power Sources* **354** 200–6
- [48] Tang H, Li W, Pan L, Tu K, Du F, Qiu T, Yang J, Cullen C P, McEvoy N and Zhang C J 2019 A robust, freestanding MXene-sulfur conductive paper for long-lifetime Li–S batteries *Adv. Funct. Mater.* **29** 1901907
- [49] Pang Q, Liang X, Kwok C Y and Nazar L F 2015 Review—the importance of chemical interactions between sulfur host materials and lithium polysulfides for advanced lithium-sulfur batteries *J. Electrochem. Soc.* **162** A2567–76

- [50] Tang H *et al* 2018 In situ formed protective barrier enabled by sulfur@titanium carbide (MXene) Ink for achieving high-capacity, long lifetime Li-S batteries *Adv. Sci.* **4** 1800502
- [51] Zhao X *et al* 2019 Antioxidants unlock shelf-stable $\text{Ti}_3\text{C}_2\text{T}_x$ (MXene) nanosheet dispersions *Matter* **1** 513–26
- [52] Limbu T B, Chitara B, Orlando J D, Garcia Cervantes M Y, Kumari S, Li Q, Tang Y and Yan F 2020 Green synthesis of reduced $\text{Ti}_3\text{C}_2\text{T}_x$ MXene nanosheets with enhanced conductivity, oxidation stability, and SERS activity *J. Mater. Chem. C* **8** 4722–31